Modeling the Pore Structure of Coal

The predictions of the random-pore model, and various other models formulated here, are compared with experimental data for the uptake of methane by coal. It is found that the most appropriate is a modified model considering coal to be comprised of microporous grains, with the random-pore model holding for the micropores in the grains. The new model still predicts the same reaction behavior as the random-pore model.

S. K. Bhatia
Department of Chemical Engineering
Indian Institute of Technology
Powai, Bombay 400 076, India

Introduction

For coal, as in all porous solids, an adequate representation of the internal structure is an important prerequisite to the successful modeling of reaction and transport processes in the solid. This is because the reaction rates are influenced by the internal surface area, which varies with conversion, and because transport parameters such as effective diffusivity and permeability are strongly pore-structure dependent. Consequently, a number of structural models have been formulated to facilitate the analysis of gas-solid reactions; however not all of the models are easily applicable to coals. The earliest of these is that of Petersen (1957), which considers the pores to be of uniform size and was originally used for the analysis of gasification behavior, although an application to the case of reactions with a solid product has also been published (Bhatia and Perlmutter, 1983). The model is, however, not suitable for coals whose pore size distribution is bimodal, often even trimodal, and cannot be represented by a uniform pore size. A more commonly used model is the grain model of Szekely and Evans (1970, 1971a), which has been successfully applied to oxide reduction (Szekely and Evans, 1971b) and to the sulfation of lime (Hartman and Coughlin, 1977) as well as to several other gas-solid systems. The model, however, predicts a monotonically decreasing surface area during gasification, while coals often show a maximum in the surface area with conversion (Hashimoto et al., 1979). In other work Hashimoto and Silveston (1973) have used a random-pore model and constructed a population balance approach to follow the modification in pore structure with conversion. However, the model contains numerous adjustable constants that are not measurable and therefore cannot be readily applied. Another model due to Simons and Finson (1979) and Simons (1979) uses several empirical relations and proposes a restrictive pore size distribution, which is not always obeyed by coals.

More recently Bhatia and Perlmutter (1980) and Gavalas (1980) have proposed a random-pore model that can predict surface area maximum with conversion, can use any arbitrary pore size distribution, and has no parameters that cannot be measured. This model has since been successfully tested for coals also by other workers (Ge et al., 1981; Su and Perlmutter, 1985; Tone et al., 1985). Yet another model has been proposed by Zygourakis et al. (1982) that considers the structure to be composed of spherical vescicles connected by cylindrical micropores. However, this model also has two or three adjustable parameters. A further anomaly is that it cannot predict penetration of the spherical macropores without diffusion through the micropores. Thus, the transient uptake of an adsorbed gas will always be particle-size dependent even if there is no concentration gradient in the macropores but there is one in the micropores. This is contrary to the findings of Nandi (1964), who observed that the diffusional uptake of gases in several coals can proceed at rates relatively independent of the particle size, suggesting gradients only in the microstructure.

Finally, Reyes and Jensen (1985) have used a random Bethe lattice model of pore structure to study the diffusion of gases in solids, and subsequently (Reyes and Jensen, 1986a, b) the gasification behavior of coal, using percolation theory. However, the structural properties such as surface area and coordination number are empirically calculated using computer simulation results for space-filling tesselations, which generally produce unreasonably high percolation thresholds. Specific expressions for the internal surface area of the Bethe lattice pore structure are lacking.

It would appear from this discussion that the random-pore model (RPM) of Bhatia and Perlmutter (1980) and Gavalas (1980) is the most suitable for coals because of the attributes mentioned above. It also meets the qualitative requirement that the macropores be penetrated independently of the micropores so that for small enough particles, size effects disappear during diffusional uptake. However, even in this case some questions arise. The model assumes that all the pores are uniformly random throughout the volume of the solid, and has successfully interpreted gasification data. However, it may well be that coal actually comprises a macropore phase and a micropore phase, with the micropores being randomly located in the latter. In

such a case if, as is usually true, the micropore surface area far exceeds the macropore surface area, then also the surface area and conversion-time behavior will follow the functional forms of the RPM in the chemically controlled regime (the regime in which it has been tested). Thus, kinetic data alone are not sufficient to distinguish between these possibilities. However, this question can be answered by a quantitative comparison of these models with diffusional uptake data such as that provided by Nandi and Walker (1970) since the predicted uptake as a function of time will be different for these cases.

It is the purpose of this paper to examine the RPM and various two-phase models of coal, all of which are expected to have similar conversion behavior in the chemically controlled regime, and to compare their predictions regarding the transient diffusional uptake of a gas with the data of Nandi and Walker. It is shown that a two-phase model which considers the solid as comprising spherical microporous grains, with the RPM holding for the micropores in each grain, gives the most adequate correlation with experimental data for various coals. The macropores in this model form the spaces between the microparticles (grains).

Pore Structure Models and Diffusion and Adsorption

In this section we examine four different pore structure models for coal: the RPM of Bhatia and Perlmutter (1980) and Gavalas (1980), and three two-phase models that consider the RPM to hold in the micropore phase, thus allowing consistency with gasification data for which the RPM has been successfully tested. The first of the two-phase models assumes that the macropores are randomly distributed in the solid, with the micropores being randomly distributed in the remainder of the solid. This is distinct from the existing RPM, which considers all pores to be randomly distributed throughout the solid. A second model considers the solid to comprise nonoverlapping microporous grains, with the macropores forming the interstitial space between the grains. The third model is a variation of the second and assumes that the solid comprises overlapping microporous grains. In the latter two cases the RPM is considered to hold in the microparticles.

Since our aim is to compare the predictions of the models regarding diffusional uptake with experimental data, we also develop here the equations for such a process for each of the pore structure models considered. In the experiments with which comparisons will be made, Nandi and Walker (1970) studied the diffusion and adsorption of methane in various coals, and reported that particle-size-related effects were not important, so that macropore diffusion was rapid and gradients existed only in the microstructure. Thus, it suffices to model only the diffusional process in the micropores for the RPM, and in the micropore phase in the other three models, neglecting gradients in the macropores. Since the difference in the models considered lies precisely in the nature of the micropore phase, comparison with the experimental data should be a good method of distinguishing between them. That macropore gradients are absent for the conditions of the experiments is also shown theoretically in the Appendix.

Random-pore model

Figure 1 depicts in two dimensions a network in which all the pores are randomly located throughout the space. As a result there are overlap regions between the small pores and large

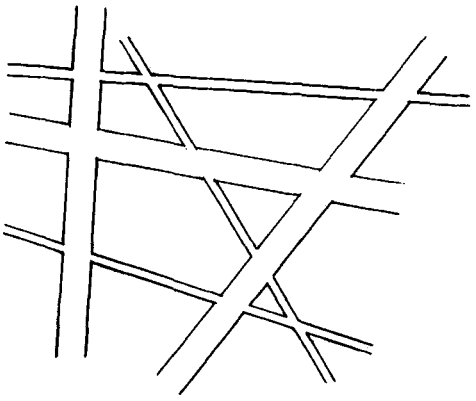

Figure 1. A random-pore network.

pores. This is the kind of model proposed by Bhatia and Perlmutter (1980) and Gavalas (1980) for gasification. The actual model of course comprises a three-dimensional network.

In writing a model for sorption under conditions of no macropore gradients, as in the experiments to be modeled, one need only consider the diffusion into the micropores. To this end we approximate the unimodal micropore size distribution by a single size, as done by Gavalas (1980) in his calculation of the micropore Thiele modulus, and write the differential balance (neglecting surface diffusion)

$$\frac{\partial C_\mu}{\partial t} + \frac{2}{r_\mu}\frac{\partial q}{\partial t} = \bar{D}\frac{\partial^2 C_\mu}{\partial Z^2} \tag{1}$$

where q is the surface concentration of the adsorbed gas in the micropore and r_μ the micropore radius. The initial and boundary conditions for this equation are

$$C_\mu = 0 \quad \text{at } t = 0 \tag{2}$$

$$C_\mu = C(t) \quad \text{at } Z = 0,\ t > 0 \tag{3}$$

$$\frac{\partial C_\mu}{\partial Z} = 0 \quad \text{at } Z = L,\ t > 0 \tag{4}$$

where $C(t)$ is the macropore gas concentration, and L is half the mean micropore length between intersections with macropores. Since there are no macropore gradients, $C(t)$ is also the external gas concentration surrounding the solid particles.

In the experiments for which sorption-time data are reported, Nandi and Walker used a constant-volume system, so that the external gas concentration changed with time. To obtain $C(t)$ it is necessary to write an overall balance

$$VC_o = VC(t) + 2V_S N_\mu \int_o^L (\pi r_\mu^2 C_\mu + 2\pi r_\mu q)\, dZ \tag{5}$$

where N_μ is the number of micropores per unit volume, and V is the volume of the external system plus the macropores of the solid. Since there are no macropore gradients this volume has been lumped with the system volume. Further, assuming equilibrium and using the linear isotherm

$$q = KC_\mu \tag{6}$$

which was found to hold for the conditions of the experiments of Nandi and Walker, Eq. 5 becomes

$$VC_o = VC(t) + 2V_s N_\mu \pi r_\mu^2 \left(1 + \frac{2K}{r_\mu}\right) \int_o^L C_\mu \, dZ \qquad (7)$$

At large time when equilibrium is attained

$$C_\mu(\infty, \lambda) = C(\infty) = C_\infty \qquad (8)$$

and Eq. 7 yields

$$C_\infty = \frac{VC_o}{V + 2\pi r_\mu^2 L \left(1 + \frac{2K}{r_\mu}\right) N_\mu V_s} \qquad (9)$$

Equation 9 may be rearranged to

$$\frac{2\pi r_\mu^2 L(1 + 2K/r_\mu) N_\mu V_s}{V} = \frac{(1 - \alpha)}{\alpha} \qquad (10)$$

where

$$\alpha = \frac{C_\infty}{C_o} \qquad (11)$$

so that Eq. 7 simplifies to

$$C^* = 1 - \frac{(1 - \alpha)}{\alpha C_o} \int_o^1 C_\mu \, d\lambda \qquad (12)$$

in which we have transformed the axial coordinate by

$$\lambda = 1 - \frac{Z}{L} \qquad (13)$$

and $C^*(t) = C(t)/C_o$. Upon defining the fractional local uptake

$$Q(t, \lambda) = C_\mu / C_\infty \qquad (14)$$

Eq. 12 simplifies to

$$C^* = 1 - (1 - \alpha) \int_o^1 Q \, d\lambda \qquad (15)$$

while Eq. 1 is transformed to

$$\frac{\partial Q}{\partial \tau} = \frac{\partial^2 Q}{\partial \lambda^2} \qquad (16)$$

where the dimensionless time τ is defined by

$$\tau = \frac{\overline{D} t}{(1 + 2K/r_\mu) L^2} \qquad (17)$$

The initial and boundary conditions for Eq. 16 are obtained by combining Eqs. 2, 3, 4, 11, 14, and 15 and are

$$Q = 0 \quad \text{at } \tau = 0, 0 \le \lambda \le 1 \qquad (18)$$

$$\frac{\partial Q}{\partial \lambda} = 0 \quad \text{at } \lambda = 0, \tau > 0 \qquad (19)$$

$$\alpha Q = 1 - (1 - \alpha) \int_o^1 Q \, d\lambda \quad \text{at } \lambda = 1, \tau > 0 \qquad (20)$$

Equations 16 and 18–20 complete the formulation of the micropore diffusion problem for the RPM under constant volume conditions. The total fractional uptake at any instant is given by

$$Q_T = \int_o^1 Q \, d\lambda \qquad (21)$$

Macropores randomly distributed in the solid, micropores in the remainder

As an alternative to the RPM one may consider the solid to be composed of randomly distributed macropores with micropores randomly located in the remainder of the solid, which becomes the micropore phase. Since the micropore surface area far exceeds the macropore surface area, under conditions of chemical control the results of the RPM as applied to gasification would still appear to hold. Figure 2 depicts the pore structure according to this model, showing no overlap between macropores and micropores.

In analyzing diffusion in the micropores of this model it is evident that there are two main directions providing the driving force, not necessarily normal to each other. One direction is along the particle radius (assuming spherical particles) and the other is normal to the local macropore surface. However, the time scale for diffusion along the former direction, $R_o^2/D_{e\mu}$, is much larger than that for the latter direction, which is $r_o^2/D_{e\mu}$, where $D_{e\mu}$ is the effective diffusivity in the microstructure and r_o is a mean macropore radius. Thus the diffusion in the microstructure will be predominantly normal to the local macropore surface and particle size effects will not be evident.

To model diffusion normal to the macropore surface it is convenient to use the concept of isoconcentration surfaces introduced by Bhatia and Perlmutter (1983) and extended by Bhatia

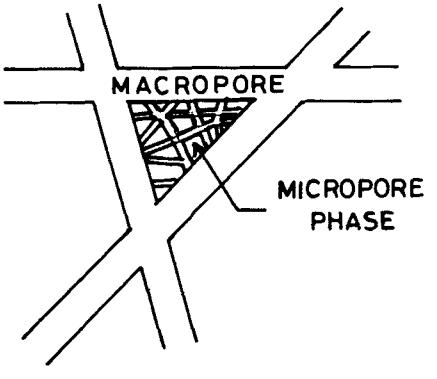

Figure 2. Model of randomly overlapping macropores with micropores randomly located in remainder of solid.

(1985). According to this concept diffusion from the macropore surface is considered to occur unidimensionally in the normal direction, yielding overlapping cylindrical surfaces of uniform concentration. The balance equation pertinent to this situation is

$$(\epsilon_\mu + KS_\mu)\frac{\partial C_\mu}{\partial t} = \frac{D_{e\mu}}{S(r)}\frac{\partial}{\partial r}\left[S(r)\frac{\partial C_\mu}{\partial r}\right] \tag{22}$$

where $S(r)$ is the area of the isoconcentration surface at a radius r. Approximating the unimodal macropore size distribution by a uniform size (r_o) and using the property of random overlapping surfaces (Bhatia and Perlmutter, 1980; Gavalas, 1980)

$$S(r) = 2\pi r L_E e^{-\pi r^2 L_E} \tag{23}$$

where L_E is the total length of the macropore axes per unit volume. The initial condition for Eq. 22 is the same as in Eq. 2 while the boundary conditions are given as

$$C_\mu = C(t) \quad \text{at } r = r_o,\ t > 0 \tag{24}$$

$$\lim_{r\to\infty}\left(\frac{\partial C_\mu}{\partial r}\right) = 0 \quad t > 0 \tag{25}$$

Introducing the transformation

$$\lambda = \frac{e^{-\pi r^2 L_E}}{e^{-\pi r_o^2 L_E}} \tag{26}$$

and combining Eqs. 22–26 results in

$$\frac{\partial C_\mu}{\partial \tau} = \frac{\partial}{\partial \lambda}\left[\lambda^2(1 - \Psi_M \ln\lambda)\frac{\partial C_\mu}{\partial \lambda}\right] \tag{27}$$

$$C_\mu = C(t) \quad \text{at } \lambda = 1,\ \tau > 0 \tag{28}$$

$$\left(\frac{\partial C_\mu}{\partial \lambda}\right) = 0 \quad \text{at } \lambda = 0,\ \tau > 0 \tag{29}$$

where the dimensionless time τ is given by

$$\tau = \frac{4D_{e\mu}t}{\Psi_M^2 r_o^2(\epsilon_\mu + KS_\mu)} \tag{30}$$

and

$$\Psi_M = \frac{4\pi L_E}{S_E^2} = \frac{1}{\pi L_E r_o^2} \tag{31}$$

is the usual structural parameter relating to the randomly overlapping macropores. The external concentration $C(t)$ is as before solved for by an overall balance:

$$VC_o = VC(t) + V_s(\epsilon_\mu + KS_\mu)\int_{r_o}^{\infty} 2\pi r L_E e^{-\pi r^2 L_E} C_\mu\, dr \tag{32}$$

which combines with Eq. 26 to yield

$$VC_o = VC(t) + V_s(\epsilon_\mu + KS_\mu)(1 - \epsilon_M)\int_o^1 C_\mu\, d\lambda \tag{33}$$

where ϵ_M is the macroporosity given, according to the properties of randomly overlapping surfaces, as

$$\epsilon_M = 1 - e^{-\pi r_o^2 L_E} \tag{34}$$

Equation 33 gives the equilibrium concentration C_∞ as

$$C_\infty = \frac{VC_o}{V + V_s(\epsilon_\mu + KS_\mu)(1 - \epsilon_M)} \tag{35}$$

which combines with Eq. 33 to yield an equation identical to Eq. 12 for the dimensionless external concentration. Introducing the fractional local uptake Q defined by Eq. 14 transforms Eq. 27 to

$$\frac{\partial Q}{\partial \tau} = \frac{\partial}{\partial \lambda}\left[\lambda^2(1 - \Psi_M \ln\lambda)\frac{\partial Q}{\partial \lambda}\right] \tag{36}$$

for which the initial and boundary conditions are clearly given by Eqs. 18–20. It is also easy to show that the total fractional uptake is still given by Eq. 21, completing the definition of the diffusion problem for this case.

Model of nonoverlapping microporous spherical grains

In this model it is assumed that the solid is composed of spherical microporous grains uniformly distributed throughout the space but without overlapping one another. Thus the macropores are defined by the intergranular space in the particles. This is similar to the model of Szekely and Evans (1970, 1971a), however we consider the grains to be microporous, as opposed to the nonporous grains of Szekely and Evans. Inside each grain the micropores are considered to be randomly overlapping, as in Figure 2. Thus, if the internal micropore surface area far exceeds the external grain surface the kinetic behavior during gasification under chemical control will still be the same as that predicted by Bhatia and Perlmutter and Gavalas. Evidence for such a model of coal exists in the work of Turkdogan et al. (1970), who studied various carbonaceous materials by microscopy and found the solids to comprise microporous polycrystalline carbon agglomerates surrounded by the larger macropores.

Diffusion and sorption in a solid defined by the model structure considered here has been previously studied by Ruckenstein et al. (1971). In the absence of concentration gradients in the macropores, the differential balance equation is

$$(\epsilon_\mu + KS_\mu)\frac{\partial C_\mu}{\partial t} = \frac{D_{e\mu}}{r^2}\frac{\partial}{\partial r}\left(r^2\frac{\partial C_\mu}{\partial r}\right) \tag{37}$$

with initial condition given by Eq. 2, and boundary conditions

$$\frac{\partial C_\mu}{\partial r} = 0 \quad \text{at} \quad r = 0,\ t > 0 \tag{38}$$

$$C_\mu = C(t) \quad \text{at} \quad r = r_g,\ t > 0 \tag{39}$$

where r_g is the grain radius, assumed uniform. Upon introducing the substitution

$$\lambda = \frac{r^3}{r_g^3} \tag{40}$$

Eq. 37 is transformed to

$$\frac{\partial Q}{\partial \tau} = \frac{\partial}{\partial \lambda}\left(\lambda^{4/3}\frac{\partial Q}{\partial \lambda}\right) \tag{41}$$

where $Q = C_\mu/C_\infty$, as defined in Eq. 14, and

$$\tau = \frac{9D_{e\mu}t}{r_g^2(\epsilon_\mu + KS_\mu)} \tag{42}$$

It is now a straightforward task to construct the balance equation for the gas in the external constant-volume system and to show that the initial and boundary conditions are given as before by Eqs. 18–20, while the total fractional uptake is given by Eq. 21.

Model of overlapping microporous spherical grains

As a variation of the previous model one may also consider the solid to be composed of overlapping microporous grains as shown in Figure 3, with the RPM holding as before for the micropores in each grain. Such a model, although considering only nonporous grains, has previously been used by Weissberg (1963) in connection with effective diffusivity calculations for macropore transport. However, our interest lies in the problem of uptake by the microstructure.

In approaching the problem of diffusion into the system of overlapping microporous spheres we utilize, as before, the concept of isoconcentration surfaces, assuming uniformly sized grains. Diffusion is therefore considered to proceed unidimensionally in a direction normal to the grain surfaces, yielding overlapping surfaces of uniform concentration. Equation 22 may then be used to model the diffusion process, with $S(r)$ representing the area of the uniform concentration surface at a radius r. As an approximation we consider these surfaces to remain as overlapping shrinking spherical surfaces as diffusion proceeds inward from the grain surfaces. Although this will not strictly be the case since some necking must occur at the overlap region of shrinking surfaces, the approximation may be used to estimate the area of the isoconcentration surface. With this approximation, for randomly overlapping spheres of radius ,

$$S(r) = 4\pi r^2 N \exp(-4\pi r^3 N/3) \tag{43}$$

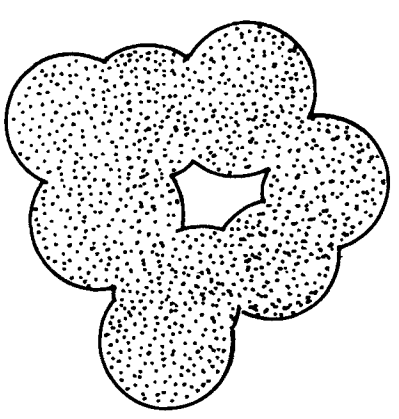

Figure 3. Model of randomly overlapping microporous spherical grains.

where N is the number density of grains. Introducing the substitution

$$\lambda = \frac{1 - \exp(-4\pi r^3 N/3)}{1 - \exp(-4\pi r_g^3 N/3)} \tag{44}$$

and combining with Eqs. 14, 22, and 43 yields

$$\frac{\partial Q}{\partial \tau} = \frac{\partial}{\partial \lambda}\left[g(\lambda)\frac{\partial Q}{\partial \lambda}\right] \tag{45}$$

where

$$\tau = \frac{9D_{e\mu}[\ln(1/\epsilon_M)]^{2/3}t}{r_g^2(\epsilon_\mu + KS_\mu)} \tag{46}$$

$$g(\lambda) = \left[\frac{1}{(1-\epsilon_M)} - \lambda\right]^2\left\{\ln\left[\frac{1}{1-\lambda(1-\epsilon_M)}\right]\right\}^{4/3} \tag{47}$$

and

$$\epsilon_M = \exp(-4\pi r_g^3 N/3) \tag{48}$$

is the macroporosity. It is not difficult to show that for this model too the initial and boundary conditions are given by Eqs. 18–20, while the total fractional uptake is given by Eq. 21.

Comparison with Experimental Data

To distinguish among the above possible models, all of which should yield similar conversion-time behavior for coal, the predictions for the fractional total uptake $Q_T(t)$ during sorption of a gas were compared with the data of Nandi and Walker (1970). These authors have reported the uptake of methane as a function of time for three different coals in a constant-volume system at 297K. For one of the coals data are presented for two different particle sizes, so that four sorption curves were available for comparison. The characteristics of the coals used are summarized in Table 1. It is seen from this table that with fine grinding the nitrogen surface area increases considerably, suggesting that some new cracks have been created, increasing the macropore surface area. As a result of these new cracks some further micropores may also be penetrated, since nitrogen is known to penetrate also some of the microstructure. Thus the surface areas reported may not be a true measure of the macropore surface. Nevertheless the smaller particles for the St. Nicholas anthracite do appear to have a significantly larger macropore area, and this leads to a different uptake curve than that observed for the larger particles.

In solving the model equations it may be noted that all four models are of the general form of Eq. 45, differing only in the functional form of $g(\lambda)$. In addition, the boundary and initial conditions are identical and are given by Eqs. 18–20. An analytical solution, however, can only be found for the RPM (the first model) and for the case of nonoverlapping spheres (the third model). However, because of the similarity of the equations and boundary conditions the same numerical scheme and computer program could be adapted quite simply for all four cases. As a result the numerical route was chosen even for those cases where analytical solution was possible. The method used was to convert

Table 1. Experimental Conditions of Nandi and Walker (1970)

Coal	Sieve Size, Tyler	Specific Volume $m^3/kg \times 10^3$	Specific Surface Area by Nitrogen $m^2/kg \times 10^{-3}$	Upper Limit for ϵ_M	α	Diffusional Parameter $D_{e\mu}/r_g^2(\epsilon_\mu + KS_\mu)$ $s^{-1} \times 10^6$
St. Nicholas anthracite	42 × 65	0.588	8	0.23	0.319	2.85
St. Nicholas anthracite	100 × 150	0.61	22.6	0.26	0.268	8.58
912 bituminous	100 × 150	0.719	2.4	0.37	0.572	12.3
888 bituminous	100 × 150	0.746	4.8	0.39	0.644	8.9

the general Eq. 45 to a system of ordinary differential equations in time by applying orthogonal collocation in the spatial variable λ. Satisfactory convergence was always obtained using eight or more collocation points. The resulting ordinary differential equations were solved using a fourth-order Runge-Kutta method.

In solving for the fractional uptake $Q_T(t)$, it is to be noted that each model involves the parameter $\alpha(= C_\infty/C_o)$. This was measured by Nandi and Walker but not specified in their paper. However, they used the values of α for each of their experiments to estimate diffusion parameters, which were specified. Using the specified diffusion parameters the actual values of α were back-calculated. These values are listed in Table 1. An additional parameter required by the second model is the macropore structural parameter which, for uniformly sized macropores, is given by (Bhatia and Perlmutter, 1981)

$$\Psi_M = \frac{1}{\ln [1/(1 - \epsilon_M)]} \tag{49}$$

Thus, both the second and fourth models effectively involved the macroporosity ϵ_M. This was not specified by the authors but its upper limit (the total porosity) was calculated from the given specific volumes assuming a conservative value of the true solid density of 2,200 kg/m^3. For distinguishing among the various models it sufficed to know only these upper limits of ϵ_M, which are given in Table 1.

Figures 4a–d show the calculated and experimental uptakes for the first model, the RPM, plotted as a function of $\sqrt{\tau/\tau_{0.5}}$, where $\tau_{0.5}$ is the dimensionless time taken to reach 50% of the maximum uptake. This way of plotting eliminates the need to know micropore diffusivity and the factor of conversion of time to dimensionless time for each model since

$$\frac{t}{t_{0.5}} = \frac{\tau}{\tau_{0.5}} \tag{50}$$

The value of $t_{0.5}$ was obtained from the smooth curves drawn by Nandi and Walker through their experimental data. Thus, for the RPM there is no adjustable parameter in the fits of Figures 4a–d. Table 2 lists the standard deviations between measured and predicted values of Q_T for each of the runs, with the standard deviation defined by

$$s = \sqrt{\frac{\sum_{i=1}^{n} (Q_{Ti} - \overline{Q}_i)^2}{n}} \tag{51}$$

where $\overline{Q}_i$ is the experimental uptake, and n is the number of data points.

When model no. 2 was used the best agreement was obtained when Ψ_M was chosen as 1, and for this value of Ψ_M the values of s were lower by about 20 to 45% than those for the RPM (model 1), as shown in Table 2. This is also evident in Figures 5a–d showing better correspondence for model 2 as compared to model 1, particularly at high uptakes. This suggests that model 2 is superior. The value of $\Psi_M = 1$, however, corresponds to $\epsilon_M = 0.63$, which is much too high. For the values of Ψ_M corresponding to the values of ϵ_M given in Table 1 the agreement was not as good and the standard deviation was higher. In actuality, since the values of ϵ_M listed are upper bounds the values of Ψ_M should be even higher than those corresponding to the listed values of ϵ_M, giving even poorer agreement. As an example, the values of the standard deviation for $\Psi_M = 5$ for the four samples are 0.0157, 0.0239, 0.0391, 0.0253, listed in the same order as in Table 2. These values are over 50% higher than the corresponding values for $\Psi_M = 1$ given in Table 1. Thus $\Psi_M = 1$ is the best choice, but this would be in disagreement with the value of Ψ_M calculated using Eq. 49 and the actual value of the macroporosity ϵ_M. This suggests that the macropores are indeed not ran-

Table 2. Standard Deviation Between Models and Experimental Data

Coal	Model 1	Model 2 ($\Psi_M = 1$)	Model 3	Model 4
St. Nicholas 42 × 65 mesh	0.0130	0.0105	0.0110	0.0181
St. Nicholas 100 × 150 mesh	0.0249	0.0230	0.0236	0.0286
912 100 × 150 mesh	0.0411	0.0227	0.0215	0.0386
888 100 × 150 mesh	0.0222	0.0163	0.0147	0.0190

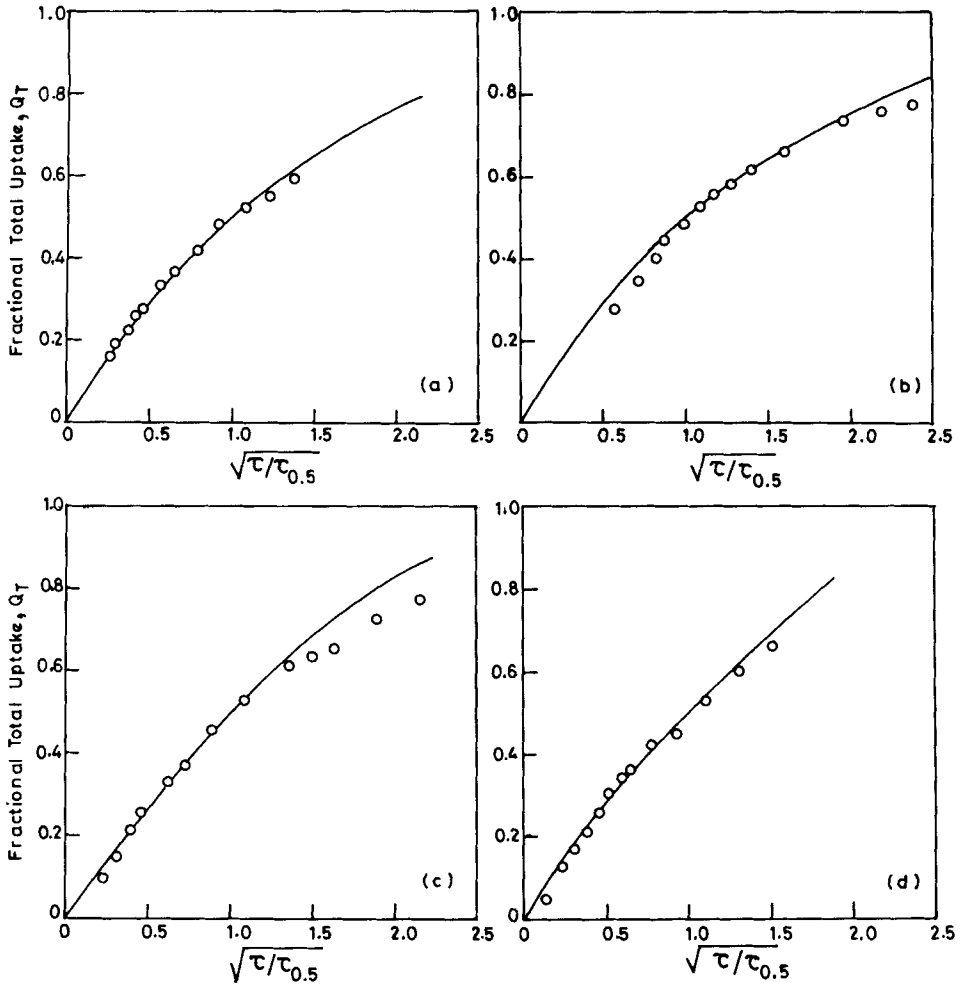

Figure 4. Experimental data and random-pore model predictions.

o Data; —— Predictions
a. 42 × 65 mesh St. Nicholas coal
b. 100 × 150 mesh St. Nicholas coal
c. 100 × 150 mesh 912 coal
d. 100 × 150 mesh 888 coal

domly distributed throughout the solid as assumed in this model.

It was shown previously (Bhatia and Perlmutter, 1980) that for $\Psi_M = 1$ the reaction surface area change during gas-solid reaction corresponds very well with the grain model. In the present work, for $\Psi_M = 1$ the isoconcentration surfaces would thus have the same area as shrinking nonoverlapping spherical surfaces. This suggests that model 3 would be just as suitable as model 2 with $\Psi_M = 1$. This is indeed true, as seen in Table 2, where no consistent difference in the standard deviations is found. Since this model has no adjustable parameter, it appears the more appropriate representation of the structure. The agreement with the data is shown in Figures 6a–d and is similar to that of model with $\Psi_M = 1$.

For model 4, involving overlapping spheres, the standard deviations are once again considerably higher, as listed in Table 2. By increasing ϵ_M the fit could be improved, but at best the agreement can be made as good as that of model 3 by setting $\epsilon_M = 1$, at which point overlap does not occur. The poorer agreement for the upper bounds of ϵ_M listed in Table 1 is also evident in Figures 7a–d particularly at high uptakes.

It appears from this examination that a model of nonoverlapping microporous spheres, with the RPM holding for the micropores within each grain, is the most appropriate for coals. However, model 2, which assumes randomly overlapping macropores with the micropores randomly situated in the remainder of the solid, with $\Psi_M = 1$, is also equally good and has some useful attributes, as discussed in the next section.

Discussion

Suggested pore structure model

In interpreting experimental data on the reaction of a porous solid, what is in question is generally not a kinetic model; rather it is an assumed model of the pore structure that is being tested. In this context the RPM appeared the most adequate model for coals, as discussed in an earlier section. All of the new models considered here would also predict the same conversion-time

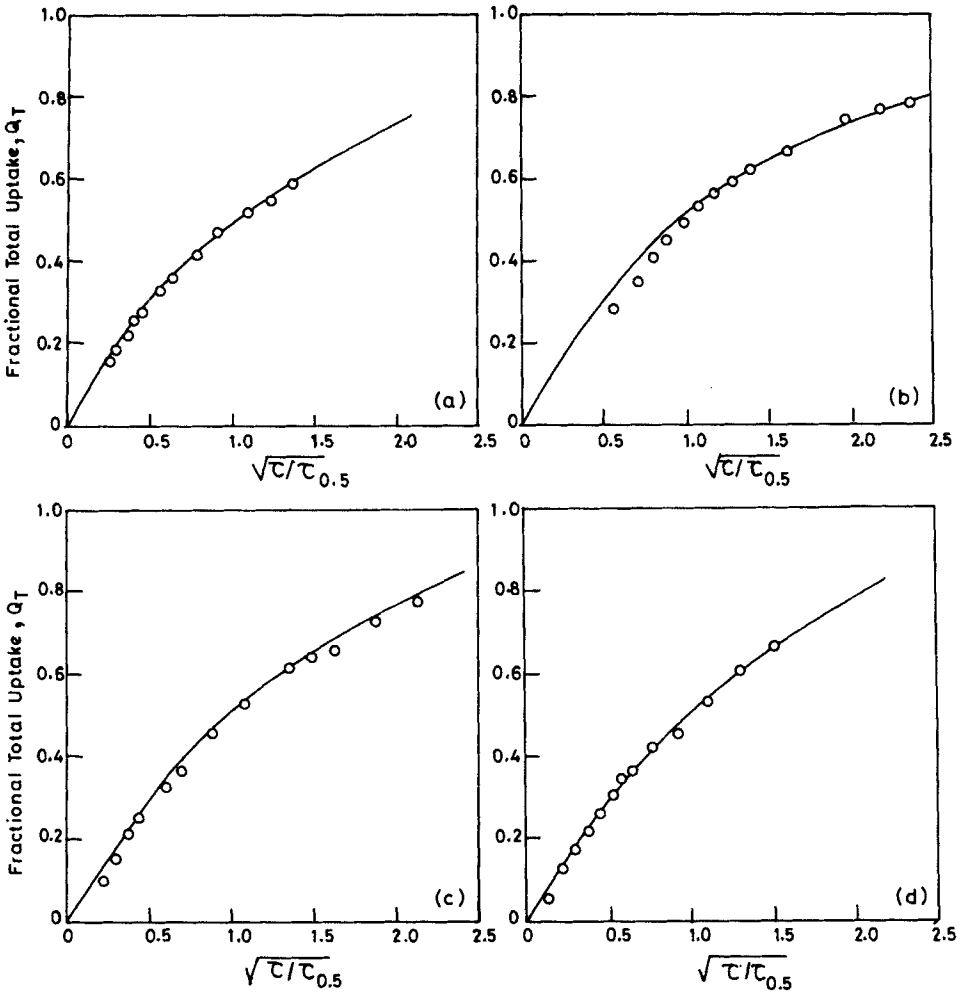

Figure 5. Experimental data and model no. 2 predictions with $\Psi_M = 1$.

o Data; —— Predictions
a. 42 × 65 mesh St. Nicholas coal
b. 100 × 150 mesh St. Nicholas coal
c. 100 × 150 mesh 912 coal
d. 100 × 150 mesh 888 coal

behavior as the RPM in the case of large micropore surface area compared to macropore surface area (as in generally true). Thus they are all serious contenders as models of coal pore structure.

A truly versatile model must, however, also successfully predict transport and other phenomena in the same porous material. Based on the present work, the model of nonoverlapping spherical microporous grains appears the most adequate. For this model, neglecting reaction on the external particle surface, the conversion-time behavior during gasification in the chemically controlled regime would still be given by the expression derived by Bhatia and Perlmutter (1980)

$$X = 1 - \left(1 - \frac{\tau}{\sigma}\right)^3 \exp\left[-\tau\left(1 + \frac{\Psi_\mu \tau}{4}\right)\right] \tag{52}$$

where the dimensionless time is given by

$$\tau = \frac{k_s C^n S_\mu t}{(1 - \epsilon_\mu)} \tag{53}$$

and the parameter σ is now related to the grain size

$$\sigma = \frac{r_g S_\mu}{(1 - \epsilon_\mu)} \tag{54}$$

In terms of the macropore surface area Eq. 54 becomes

$$\sigma = \frac{3(1 - \epsilon_M) S_\mu}{(1 - \epsilon_\mu) S_M} \tag{55}$$

For coals where the micropore surface area is several times (often 10 or more times) the macropore surface area, σ will usually be larger than 20. As shown in Bhatia and Perlmutter (1980), for such large values of σ the grain size effect is unimportant and Eq. 54 reduces in the limit $\sigma \to \infty$ to

$$X = 1 - \exp\left[-\tau\left(1 + \frac{\Psi_\mu \tau}{4}\right)\right] \tag{56}$$

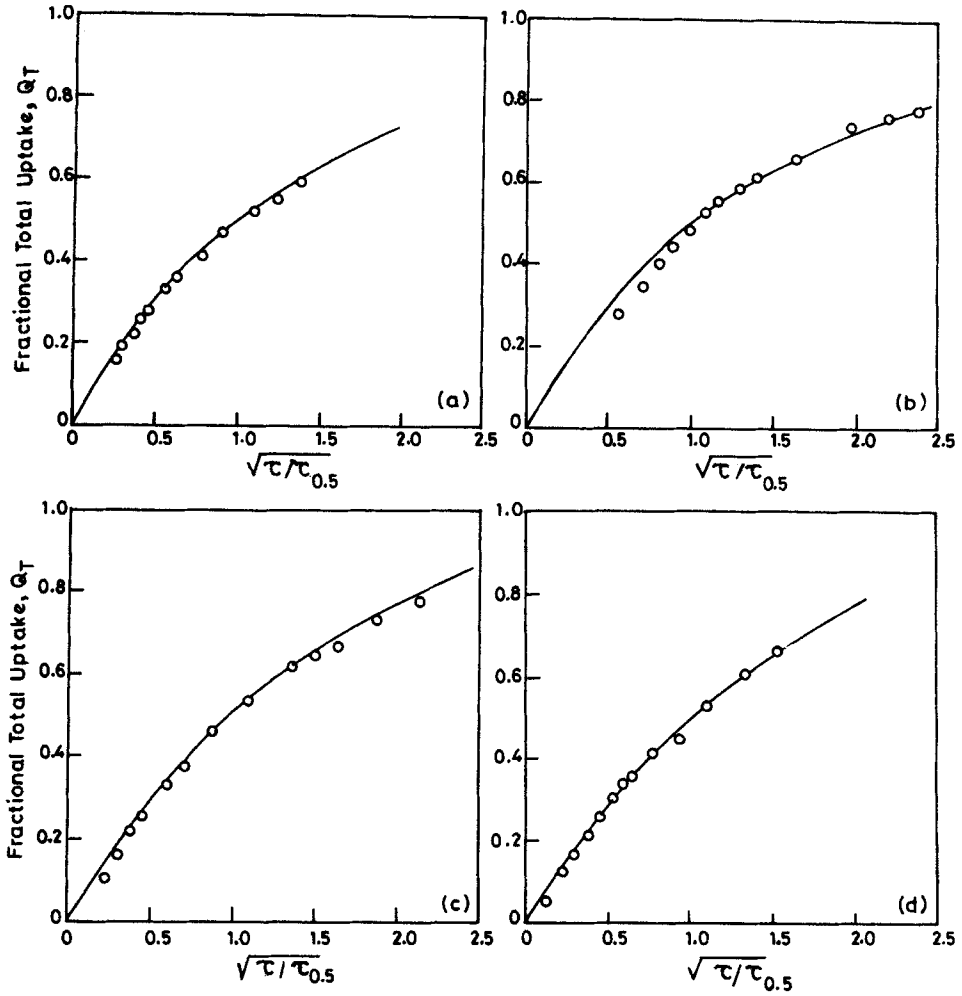

Figure 6. Experimental data and model no. 3 predictions.

o Data; —— Predictions
a. 42 × 65 mesh St. Nicholas coal
b. 100 × 150 mesh St. Nicholas coal
c. 100 × 150 mesh 912 coal
d. 100 × 150 mesh 888 coal

which yields

$$\frac{dX}{d\tau} = (1 - X)\sqrt{1 - \Psi_\mu \ln(1 - X)} \qquad (57)$$

the precise expressions that have been tested (Bhatia and Perlmutter, 1980; Gavalas, 1980; Ge et al., 1981; Tone et al., 1985; Su and Perlmutter, 1985).

Since model 2 with $\Psi_M = 1$ also fits the uptake data equally well and will yield the same expressions as in Eqs. 56 and 57 for the conversion in the chemically controlled regime, it also appears to be a useful alternative. It will be particularly attractive for gasification in the diffusion regime, where it is necessary to predict the change in effective macropore diffusivity with conversion. Since the effective diffusivity depends upon pore radius (for Knudsen diffusion controls transport in coal macropores) model 2, which can predict changes in pore radius with conversion, becomes especially useful. This same attribute cannot be ascribed to the microporous grain model, which instead yields changes in grain size with conversion. Thus, for practical reasons model 2 with $\Psi_M = 1$ may be chosen for solving gasification problems, since it will still yield the same variation in macropore surface area as well as conversion-time behavior.

It should be mentioned here that a model of microporous grains is also effectively the one used by Nandi and Walker for extracting diffusion parameters from their data. However, they only used initial slopes and made no parameter-free comparison of the model predictions and data as presented here. Thus the model was not tested and there was no clear reason for its choice.

Deviation between theory and experiment

While it is clear from Table 2 that the microporous grain model or model 2 with $\Psi_M = 1$ are the most suitable under all conditions, some statement is necessary regarding the deviation between the data and model predictions. Most likely the small deviations evident in Figures 6a–d are due to the assumption of a linear isotherm, Eq. 6. Over the pressure range used the isotherms reported by Nandi and Walker are indeed approxi-

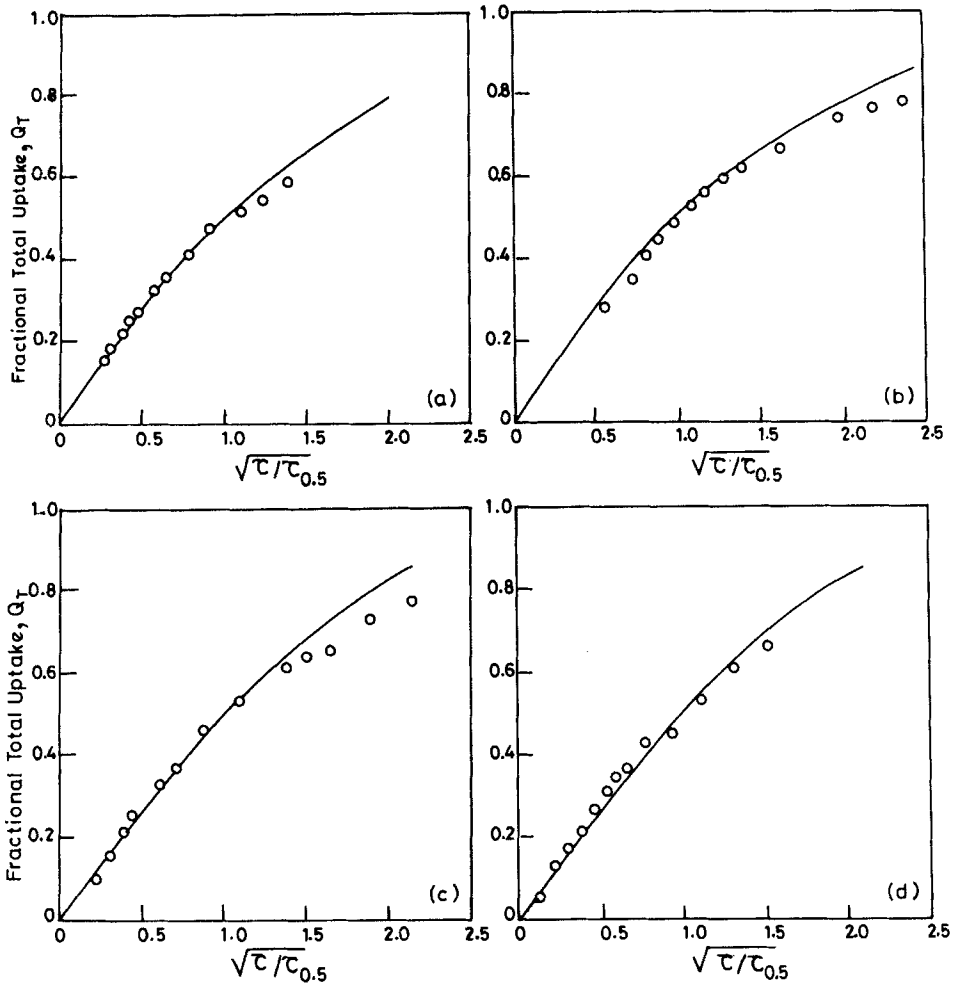

Figure 7. Experimental data and predictions using model of overlapping microporous grains.

o Data; —— Predictions
a. 42 × 65 mesh St. Nicholas coal
b. 100 × 150 mesh St. Nicholas coal
c. 100 × 150 mesh 912 coal
d. 100 × 150 mesh 888 coal

mately linear, but with some deviation at the higher pressures. This may account for the deviation between experiment and theory, for at small times the external pressure would be in the nonlinear region for the constant-volume system used. It is essentially in the small times that the error is the largest, as seen in the figures.

Calculation of effective micropore diffusivities

While we have presented here the correspondence between model and data, it was not possible to estimate accurately the values of the effective diffusivities in the microporous grains. This was because the grain sizes and microporosities were not accurately known. However, the diffusional parameter $D_{e\mu}/r_g^2(\epsilon_\mu + KS_\mu)$ could be calculated from the theoretical time $\tau_{0.5}$ and the actual time $t_{0.5}$. The results are given in Table 1. The difference between the values for the two samples of St. Nicholas coal cannot be ascribed to particle size effects, because when one allows for the fact that the grain size of the larger particles is almost three times that of the smaller (as seen from the nitrogen surface areas), the value of $D_{e\mu}/(\epsilon_\mu + KS_\mu)$ for the larger particles is higher by a factor of three. This is exactly the reverse of what might be expected if macropore diffusion and particle size effects were important. Most likely this difference is due to the penetration of the micropores by nitrogen, yielding inaccurate macropore surface areas and grain sizes. A further, theoretical, demonstration that macropore gradients are absent is provided in the Appendix.

Although the effective micropore diffusivities could not be calculated accurately, the value estimated in the Appendix for the 100 × 150 mesh sample of the St. Nicholas coal suggests that they are of the order of 10^{-19} to 10^{-18} m^2/s at 297K. This is more than 10 orders of magnitude lower than that expected if Knudsen diffusion were the controlling mechanism, suggesting some other form of diffusion. Although there is some uncertainty in the value of the effective micropore diffusivity, because of the lack of a precise estimate of grain size the error is unlikely to be more than one order of magnitude, and certainly much smaller than a factor of 10^{10}. Consequently, the invalidity of the Knudsen mechanism of diffusion under these conditions is not in doubt, and this is consistent with prior interpretations (Nandi and Walker, 1970) of the diffusion at around room tempera-

tures being activated. Calculations of the micropore Thiele modulus and effectiveness factor for char gasification under high-temperature conditions (Bhatia, 1981; Gavalas, 1980), however, assume a Knudsen mechanism of diffusion. Further studies of diffusion in coal chars under nonreactive conditions, but at the high temperatures typical of gasification, would therefore appear to be desirable in order to resolve this issue and determine the mechanism operating under such conditions.

Notation

$C_M^* = C_M/C_o$
C, C_M = gas concentration in macropores
C_μ = gas concentration in micropores
C_o = initial gas concentration in system
C_∞ = gas concentration at equilibrium
D = micropore diffusivity
D_{eM} = effective diffusivity in macropore regions
$D_{e\mu}$ = effective diffusivity in micropore phase
K = equilibrium constant
L = micropore length
L_E = total length of macropore axes per unit volume
n = number of data points
N = number of grains per unit volume
N_μ = number of micropores per unit volume
q = surface concentration of adsorbed gas
Q = fractional local uptake
Q_T = fractional total uptake
Q_I = experimental fractional uptake
Q_{TI} = predicted fractional uptake
r = radius
r_o = macropore radius
r_g = grain radius
r_μ = micropore radius
R = radial location in particle
R_o = particle radius
s = standard deviation
$S(r)$ = area of isoconcentration surface at radius r
S_M = macropore surface area per unit volume
S_μ = micropore surface area per unit volume of micropore phase
t = time
V = system volume
V_s = sample volume
X = conversion
Z = axial location in pore

Greek letters

$\alpha = C_\infty/C_o$
β = defined in Eq. A3
δ = defined in Eq. A4
ϵ_μ = micropore volume per unit volume of micropore phase
$\eta = R/R_o$
$\Psi_M = 1/(\pi L_E r_o^2)$, structural parameter for macropores
Ψ_μ = structural parameter for micropores
σ = defined in Eq. 54
ρ_b = particle density
τ = dimensionless time
λ = dummy variable

Appendix: Criteria for Absence of Macropore Concentration Gradients

Since we have assumed no macropore diffusional limitations for the experimental conditions of Nandi and Walker (1970), it is necessary to develop criteria for the validity of this hypothesis. To this end we consider the macropore diffusion equation

$$(\epsilon_M + KS_M)\frac{\partial C_M}{\partial t} = \frac{D_{eM}}{R^2}\frac{\partial}{\partial R}\left(R^2\frac{\partial C_M}{\partial R}\right) - \frac{3(1-\epsilon_M)}{r_g} D_{e\mu}\left(\frac{\partial C_\mu}{\partial r}\right)_{r=r_g} \quad \text{(A1)}$$

in which we have considered spherical particles, and used model no. 3 (the microporous grain model) for the solid structure. Since we intend to show that only micropore diffusional limitations exist, time is to be made dimensionless through Eq. 42, and Eq. A1 yields

$$\beta\frac{\partial C_M^*}{\partial \tau} = \frac{1}{\eta^2}\frac{\partial}{\partial \eta}\left(\eta^2\frac{\partial C_M^*}{\partial \eta}\right) - \delta\left(\frac{\partial Q}{\partial \lambda}\right)_{\lambda=1} \quad \text{(A2)}$$

where

$$\beta = \frac{9D_{e\mu}(\epsilon_M + KS_M)R_o^2}{r_g^2(\epsilon_\mu + KS_\mu)De_M} \quad \text{(A3)}$$

$$\delta = \frac{9D_{e\mu}R_o^2\alpha(1-\epsilon_M)}{r_g^2 D_{eM}} \quad \text{(A4)}$$

and we have used the substitution in Eq. 40. To demonstrate the absence of macropore diffusional limitations it suffices to show that both β and δ are negligibly small compared to unity. For this purpose it is necessary to have estimates of K, r_g, S_μ, $D_{e\mu}$, and D_{eM}.

We consider here the 100 × 150 mesh St. Nicholas coal for which adsorption isotherms at 297K have been provided by Nandi and Walker. At equilibrium, neglecting adsorption on macropore surfaces,

$$KC = \frac{\bar{\eta}\rho_b}{22.405 \times S_\mu(1-\epsilon_M)}$$

where $\bar{\eta}$ is the volume of gas at NTP adsorbed per unit mass of solid (m^3 NTP/kg) and ρ_b the bulk density of the solid. The data of Nandi and Walker yield $\bar{\eta} \simeq 0.017$ m^3 NTP/kg at 5.26 atm of methane at 297K. Thus, for the 100 × 150 mesh particles, for which $\rho_b = 1{,}640$ kg/m^3, $KS_\mu = 6.78$, assuming a macroporosity of 0.15. For the 100 × 150 mesh particles $t_{0.5} = 423.5$ s from the experimental data, while $\tau_{0.5} = 0.0327$ from the model. Using Eq. 42,

$$0.0327 = \frac{9D_{e\mu} \times 423.5}{r_g^2(\epsilon_\mu + KS_\mu)}$$

therefore

$$\frac{D_{e\mu}}{r_g^2} = 5.9 \times 10^{-5}\text{s}^{-1} \quad \text{(A5)}$$

in which we have taken the microporosity of the grains, ϵ_μ, as 0.1. To calculate D_{eM} we estimate a macropore radius as

$$r_o = \frac{2\epsilon_M}{S_M}$$

Taking $\epsilon_M = 0.15$, and $S_M = 22.6 \times 10^3 \rho_b$ m^{-1}, gives $r_o = 8.09 \times 10^{-9}$ m. For this pore radius the Knudsen diffusivity at 297K is $D_M = 3.38 \times 10^{-6}$ m^2/s, which gives $D_{eM} = 1.69 \times 10^{-7}$ m^2/s, assuming

$$D_{eM} = \frac{\epsilon_M D_M}{3}$$

in which we have taken the tortuosity as 3. The above information, along with the mean size $R_o = 6.28 \times 10^{-7}$ m for 100 × 150 mesh particles, is sufficient to calculate δ, which turns out to be 2.8×10^{-6}, since $\alpha = 0.268$ for the run.

To calculate β we assume that the macropore surface area is one-tenth the micropore surface area, yielding $(\epsilon_M + KS_M) = 0.83$. This yields $\beta = 1.5 \times 10^{-6}$. Thus, both β and δ are negligible compared to unity and macropore diffusional limitations are absent. Following this method it is straightforward to show the same for all the four experiments and each of the models used here.

As a point of interest we estimate here the approximate micropore diffusivity using Eq. A5 and

$$r_g = \frac{3(1 - \epsilon_M)}{S_M}$$

Taking $S_M = 22.6 \times 10^3 \rho_b$ m^{-1}, gives $r_g = 6.88 \times 10^{-8}$ m, and $D_{e\mu} = 2.8 \times 10^{-19}$ m^2/s.

Literature Cited

Bhatia, S. K., "Effect of Pore Structure on the Kinetics of Fluid-Solid Reactions," Ph.D. Thesis, Univ. Pennsylvania (1981).

———, "Analysis of Distributed Pore Closure in Gas-Solid Reactions," *AIChE J.*, **31**, 642 (1985).

Bhatia, S. K., and D. D. Perlmutter, "A Random-Pore Model for Fluid-Solid Reactions.I: Isothermal, Kinetic Control," *AIChE J.*, **26**, 379 (1980).

———, "The Effect of Pore Structure on Fluid-Solid Reactions: Application to the SO_2-Lime Reaction," *AIChE J.*, **27**, 226 (1981).

———, "Unified Treatment of Structural Effects in Fluid-Solid Reactions," *AIChE J.*, **29**, 281 (1983).

Gavalas, G. R., "A Random Capillary Model with Application to Char Gasification at Chemically Controlled Rates," *AIChE J.*, **26**, 577 (1980).

Ge, C., S. Kimura, S. Tone, and T. Otake, "Gasification of Coal Char with Steam. 2: Pore Structure and Reactivity," *J. Japan Petrol. Inst.*, **24**, 344 (1981).

Hartman, M., and R. W. Coughlin, "Reaction of Sulfur Dioxide with Limestone and the Grain Model," *AIChE J.*, **23**, 353 (1977).

Hashimoto, K., K. Miura, F. Yoshikawa, and I. Imai, "Change in Pore Structure of Carbonaceous Materials During Activation and Adsorption Performance of Activated Carbon," *Ind. Eng. Chem. Process Des. Dev.*, **18**, 73 (1979).

Hashimoto, K., and P. L. Silveston, "Gasification. I: Isothermal Kinetic Control Model for a Solid with a Pore Size Distribution," *AIChE J.*, **19**, 259 (1973).

Nandi, S. P., Ph.D. Thesis, Pennsylvania State Univ. (1964).

Nandi, S. P., and P. L. Walker, "Activated Diffusion of Methane in Coal," *Fuel*, **49**, 309 (1970).

Petersen, E. E., "Reaction of Porous Solids," *AIChE J.*, **3**, 443 (1957).

Reyes, S., and K. F. Jensen, "Estimation of Effective Transport Coefficients in Porous Solids Based on Percolation Concepts," *Chem. Eng. Sci.*, **40**, 1723 (1985).

———, "Percolation Concepts in Modeling of Gas-Solid Reactions. I: Application to Char Gasification in the Kinetic Regime," *Chem. Eng. Sci.*, **41**, 333 (1986a).

———, "Percolation Concepts in Modeling of Gas-Solid Reactions. II: Application to Char Gasification in the Diffusion Regime," *Chem. Eng. Sci.*, **41**, 345 (1986b).

Ruckenstein, E., A. S. Vaidyanathan, and G. R. Youngquist, "Sorption by Solids with Bidisperse Pore Structures," *Chem. Eng. Sci.*, **26**, 1305 (1971).

Simons, G. A., "The Structure of Coal Char. II: Pore Combination," *Combust. Sci. Tech.*, **19**, 227 (1979).

Simons, G. A., and M. L. Finson, "The Structure of Coal Char. I: Pore Branching," *Combust. Sci. Tech.*, **19**, 217 (1979).

Su, J. L., and D. D. Perlmutter, "Effect of Pore Structure on Char Oxidation Kinetics," *AIChE J.*, **31**, 973 (1985).

Szekely, J., and J. W. Evans, "A Structural Model for Gas-Solid Reactions with a Moving Boundary," *Chem. Eng. Sci.*, **25**, 1091 (1970).

———, "A Structural Model for Gas-Solid Reactions with a Moving Boundary. II," *Chem. Eng. Sci.*, **26**, 1901 (1971a).

———, "Studies in Gas-Solid Reactions. II: An Experimental Study of Nickel Oxide Reduction with Hydrogen," *Met. Trans.*, **2**, 1699 (1971b).

Tone, S., S. Kimura, Y. Hino, and T. Otake, "Potassium-Catalyzed Steam Gasification of Coal Char in a Pressurized Stream of H_2O-H_2-CO Mixture Gas," *J. Chem. Eng. Japan*, **18**, 131 (1985).

Turkdogan, E. T., R. G. Olsson, J. V. Vinters, "Pore Characteristics of Carbons," *Carbon*, **8**, 545 (1970).

Weissberg, H. L., "Effective Diffusion Coefficients in Porous Media," *J. Appl. Phys.*, **34**, 2636 (1963).

Zygourakis, K., L. Arri, and N. R. Amundson, "Studies on the Gasification of a Single Char Particle," *Ind. Eng. Chem. Fundam.*, **21**, 1 (1982).

Manuscript received Nov. 24, 1986, and revision received Mar. 17, 1987.